Contents lists available at ScienceDirect

Microchemical Journal

journal homepage: http://ees.elsevier.com

Rubens' painting as inspiration of a later tapestry: Non-invasive analyses provide insight into artworks' history

Alice Dal Fovo [a,*], J. Striova [a], E. Pampaloni [a], A. Fedeli [b], M.M. Morita [c], D. Amaya [c], F. Grazzi [d], M. Cimò [e], C. Cirrincione [e], R. Fontana [a]

[a] CNR-INO National Institute of Optics, National Research Council, Largo E. Fermi 6, 50125 Florence, Italy
[b] Università della Calabria, Dipartimento di Biologia, Ecologia e Scienze della Terra, 87036 Rende, Cosenza, Italy
[c] Centro de Investigaciones Ópticas, CONICET-UNLP-CICBA, P.O. Box 3, 1897 Gonnet, Argentina
[d] CNR-IFAC Institute of Applied Physics Nello Carrara, National Research Council, Via Madonna del Piano 10, 50019 Sesto Fiorentino, Florence, Italy
[e] OPD Opificio delle Pietre Dure, Via degli Alfani 78, 50122 Florence, Italy

ARTICLE INFO

Keywords
Tapestry
Painting
Spectral correlation mapping
Raman spectroscopy
Near infrared reflectography
3D analysis

ABSTRACT

The 17th century painting *Madonna della Cesta* by Rubens and its presumed textile reproduction created by Févère for the House of Medici were analysed in comparison. A number of non-invasive optical techniques were applied with the aim to identify similarities and differences between tapestry and painting, in order to shed light on a possible link between their respective authors. The use of a multi-analytical approach proved effective for the acquisition of iconographic, morphological, structural, and compositional information for a comprehensive characterization of the two artworks. While serving as relevant support for documentation and conservation purposes, data so obtained also provide evidence of the uncanny resemblance between the two artworks, and specifically suggest the use by Févère of the same large-scale preparatory drawing (carton) realized by Rubens for his oil painting.

1. Introduction

During the Renaissance period the manufacture of tapestries flourished throughout Europe, as these artworks increasingly served as indicators of political and cultural status – mainly because of the precious materials they were made of and their overall production costs. Tapestry manufacture peaked in Florence in the second half of the sixteenth century during the reign of Cosimo I, under the influence of Flemish artisans Nicholas Karcher and Jan Rost. Their working technique relied primarily on the horizontal weaving of threads on low-warp looms (*basse-lisse*), which drastically reduced production time and costs [1]. Tapestry manufacture intensified over the following 80 years in order to address an increasing market demand, which revolved around tapestries functional rather than decorative value. At this point, a further technical innovation was introduced by French weaver Pietro Févère (also known as Pierre Le Fevre), who was appointed chief tapestry master in 1630 by the Grand Duke of Tuscany, Ferdinando II de' Medici. Févère perfected the use of vertical looms (*haute-lisse*), which allowed for greater accuracy and higher quality, but at the same time required longer production times compared to horizontal weaving techniques. Févère's artworks were matched only by his rival Pietro van Asselt's production, and soon the two monopolised the tapestry market, each claiming the superiority of their respective weaving methods [2]. Such claims, however, are considered unsubstantial today, since there is no recognizable difference in the texture or conservation of textiles made with *haute* or *basse lisse*, as witnessed by the tapestry series *The Seasons* (1640–1643), which was jointly manufactured by both Févère and van Asselt, based on model paintings by Michelangelo Cinganelli, and now property of the Province of Siena. More specifically, the *Autumn* and *Summer Seasons*, weaved by Févère with the vertical loom, and the *Spring* and *Winter Seasons*, weaved by van Asselt with the low loom, display no evident difference except for the selection of colours and materials. While Févère used to combine wool with silk and enhance the spatial layout of his scenes with abundant golden silver and vibrant tone contrasts, van Asselt used mostly wool for the background, which resulted in flattened, theatre-backdrop-like spaces with less vivid colours.

It was in those same years that weaving artists started to use large-scale preparatory drawings or paintings, named cartons, which introduced significant innovations in the way tapestry subjects and scenes

* Corresponding author.
E-mail address: alice.dalfovo@ino.it (A. Dal Fovo)

https://doi.org/10.1016/j.microc.2019.104472
Received 31 August 2019; Received in revised form 28 October 2019; Accepted 27 November 2019
Available online xxx
0026-265/

were represented, eventually turning these decorative fabrics into fully-fledged textile paintings. Italian mannerists Pontormo, Bronzino, and Salviati, authored such exquisite cartons, which were soon considered artworks in their own right, and as such preserved and restored in case of damage [1]. At European level, tapestry manufacture was greatly influenced by Peter Paul Rubens' work, whose sketches and oil-painted cartons depicted the entire design of tapestries, from the use of colour, to the distribution of light and shadow, and were then faithfully reproduced in wool and silk [3].

Scientific diagnostics currently conducted on tapestries focus on the identification of organic dyes used for textile colouring [4,5]. Colorants' high sensitivity to light represents one of the main causes of tapestry deterioration, which is why tapestry degradation processes are investigated by means of non-invasive spectroscopic techniques prior and as support to restoring interventions [6,7]. As regards textile characterization, near infrared (NIR) spectroscopy has been successfully applied to fabrics' identification and mapping analysis [8], specifically aimed at determining textiles' moisture content as potential age-related marker [9].

The tapestry analysed in this study was made by Févère between 1652 and 1654 and belongs to a private collection. It is believed to be based on Rubens' 1615 oil painting *Madonna della Cesta* [Madonna of the Basket], currently displayed at the Galleria Palatina in Florence. Although there is no evidence attesting the use of cartons, the resemblance of the tapestry and painting motif is uncanny, especially when considering the different substrates composing the two artworks. Both artworks were hosted at the Opificio delle Pietre Dure (OPD) for conservation and/or documentation purposes. These operations included a series of analyses carried out at the National Research Council - National Institute of Optics (CNR-INO) by means of non-invasive optical techniques, such as micrometric characterization of superficial and structural morphology through the application of 3D scanning methods (i.e. laser scanning microprofilometry [10] and multi-spectral scanning [11,12]), and analysis of constituting materials, such as pigments and supports, by means of Spectral Correlation Mapping (SCM) [13], Fibre Optics Reflectance Spectroscopy (FORS) [14], and Raman spectroscopy [15]. Since analyses conducted on the tapestry's structure and morphology may yield useful insights into its production process, they may also highlight the potential influence of other artworks on the depicted subjects. To our knowledge, studies investigating the link between a painting and its presumed textile copy are unprecedented in the relevant literature. The aim of this study was therefore to apply the multi-analytical approach for a comprehensive understanding of both artworks, identifying possible similarities and differences from both iconographic and compositional point of view, in order to shed light on the link between their respective authors.

2. Instruments

2.1. Multi-spectral Vis-NIR scanning

The artworks were examined with a multi-spectral Vis–NIR scanner developed by the INO Heritage Science Group for *in Situ* analysis [16,17]. The scanner works in the visible (380 - 750 nm range, 20 - 30 nm spectral resolution) and in the near infrared regions (750 - 2500 nm range, 50 - 100 nm spectral resolution), generating single-point spectral data and 32 high-definition monochromatic images of the analysed surface (16 images in the visible and 16 in the NIR). The motorized stage for axial displacement (perpendicular to the painting surface) moves with a step of 250 μm and speed of 25 mm/s. The scanner's autofocus system, based on a high-speed triangulation distance metre and a custom-made control software, ensures optimal target-lens distance during scanning, which results in a set of perfectly superimposing monochromatic images, free from aberrations and metrically correct [18].

2.2. Laser scanning microprofilometry

Morphological analysis was carried out by means of a laser scanning micro-profilometer [19], which was specifically developed for measurements on a wide range of materials and surfaces, regardless of their chromatic, reflective, and diffusion properties [20,21]. A commercial conoprobe (Optimet, Conoprobe 1000) is set up on the scanning device, which is composed of two perpendicularly mounted high-precision motorized linear stages, allowing for measurements on a maximum area of 30×30 cm^2. The profilometer has 1 μm axial resolution, 20 μm lateral resolution, and 8 mm dynamic range. The output is a faithful, high-resolution topographic map of the measured surface, which may be displayed either as a 3D model or as a flat image. The latter may be further processed through the application of digital filters and rendering techniques, in order to enhance micrometric details and improve their readability.

2.3. Fibre optics reflectance spectroscopy (FORS)

FORS spectra were acquired with a Zeiss Multi-Channel Spectrometer (MCS), comprising a MCS521 VIS NIR - extended module and a MCS511 NIR 1.7 module with spectral sensitivity set within ranges of 304 - 1100 nm and 950 - 1700 nm and spectral resolution of 3.2 nm and 6.0 nm, in the visible and IR region, respectively. Three measurement points were selected for every sample, with each spectrum averaged over three acquisitions for each measurement, for a total of nine acquisitions per point, using a 45°/0° illumination/observation geometry and a 100% reflecting reference (Spectralon). The output signal was processed through a dedicated software, providing also CIEL*a*b* coordinates with standard D65 illuminant and 2° observer [22].

2.4. Raman spectroscopy

Two commercial devices were used for Raman analysis at two different points in time, depending on the availability of the analysed artworks. The tapestry was analysed with a BWTEK I-Raman Plus, a portable instrument equipped with a laser emitting at a wavelength of 785 nm with 2 cm^{-1} resolution in the 60–3180 cm^{-1} range (a range that covers all main energy transitions of most molecular systems present in cultural heritage objects). The instrument is equipped with a measuring head, including various microscope objectives and a camera collinear with the source, which enables direct observation of the analysed area and tailored selection of the most significant pigment or dye grains.

The painting was analysed with a portable Raman Bruker Bravo Spectrophotometer, equipped with a double excitation laser at 785 and 853 nm (Duo LASER™), whose high sensitivity extends across a wide spectral range, from 300 to 3200 cm^{-1}. The signal acquired from each excitation wavelength is detected by the charge-coupled device (CDD) and processed by a dedicated software (OPUS) in two different spectral ranges, 300–2200 cm^{-1} and 1200- 3200 cm^{-1}, respectively. The device uses a patented fluorescence mitigation algorithm (SSE™, Sequentially Shifted Excitation) allowing for the automatic removal of fluorescence, which may otherwise interfere with the Raman signal [23].

3. Methods

3.1. Spectral correlation mapping (SCM)

Spectral data acquired with Vis-NIR scanning were used to compute the spectral correlation mapping (SCM) of both artworks' surfaces, based on similarities between spectral images and reference spectrum [24,25]. SCM relies on the spectral correlation function (SCF) algorithm, which allows for the identification of differences between data

cubes that are otherwise undetectable [13]. SCM represents an improvement of SAM (Spectral Angle Mapper), which calculates the angles formed between reference and image spectrum. The latter are treated as vectors in a space with dimensionality equal to the number of bands, taking into account the derivative of the Pearsonian Correlation Coefficient that eliminates negative correlation, while preserving SAM's shading effect minimization.

3.2. 3D coloured models

3D coloured models of selected areas were obtained by merging the topographic maps and RGB images generated by the multi-spectral scanner. Given the different spatial sampling used for the acquisition of the topographic maps (50 μm) and the RGB images (250 μm), processing necessarily involved the application of bilinear interpolation to each image's colour information. Point clouds were processed with a Poisson Surface Reconstruction [26] filter in the MeshLab© software system [27]. The Mutual information algorithm was used for the registration of colour images in an iterative optimization framework [28], whereas colour information data were projected on the 3D meshes, thus obtaining a colour per vertex 3D model.

4. Results and discussion

4.1. Iconographic analysis - Multi-spectral Vis-NIR scanning

Correspondence between the depicted subject was observed by superposing the RGB images of Rubens' painting (Fig. 1a) and Févère's tapestry (Fig. 1b), after the images had been reconstructed from VIS channels using standard D65 illuminant and 2° observer. The natural warping of the tapestry was simulated through the application of an elastic image-matching algorithm to the tapestry image. Two-dimensional warping was performed by treating a number of preselected portions of the image as nearly rigid objects (central part of the tapestry), while elastically deforming the rest of the image (frame). The correspondence observed through the geometrical overlap of the two artworks (Fig. 1c) seems to suggest that Fevère did refer to the same large-scale preparatory drawing (carton) used by Rubens for his oil painting. As regards the minor differences in the contours of the depicted figures, we believe that they may be attributed to the tapestry's slight deformation, due to its long-time vertical hanging.

Fig. 2 highlights the only significant difference between the two artworks at preparatory stage, namely a *pentimento* which is only visible in the comparison between the painting and its underpainting: indeed, the NIR image at 1600 nm reveals that the basket, cradling Baby Jesus and giving the painting its current name, was initially smaller in size and lacking the angel-like decoration detail, which was added in the final version of the painting. Imaging analyses of Févère's tapestry, however, seem to indicate that the size and decoration of the basket were based on the painting rather than its preliminary underpainting. The same seems to hold true as regards a detail of St. John's clothing in the lower left corner of the artwork: while it appears to be part of Rubens' underpainting, it is missing in the painting itself, as well as in the tapestry design.

4.2. Structural and morphological analysis

4.2.1. Multi-spectral Vis-NIR scanning

Rubens' wooden panel morphology was analysed as raw structure by means of multi-spectral scanning: the three-dimensional map of the painting (Fig. 3b) was first acquired through the generation of a set of vertical profiles, which were then processed to obtain a low-resolution topographic map of the artwork's surface. The painting's 3D map shows numerous deformations possibly due to variations of environmental parameters, such as temperature and humidity. The three wooden panels

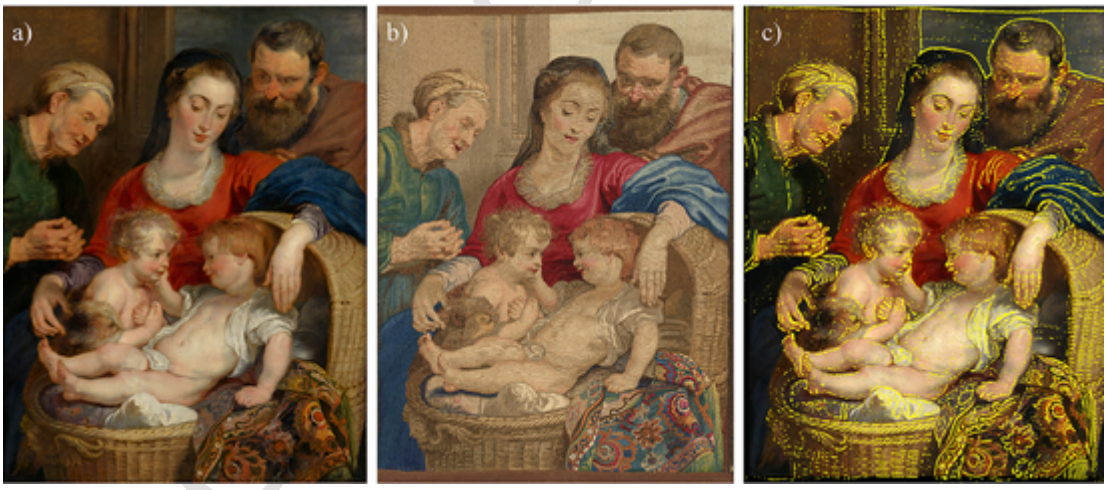

Fig. 1. Multispectral analysis of *Madonna della Cesta* oil painting by Rubens (a) and tapestry by Févère (b); superimposition of the tapestry motif (in yellow) on Rubens' painting after elastic transformation (c).

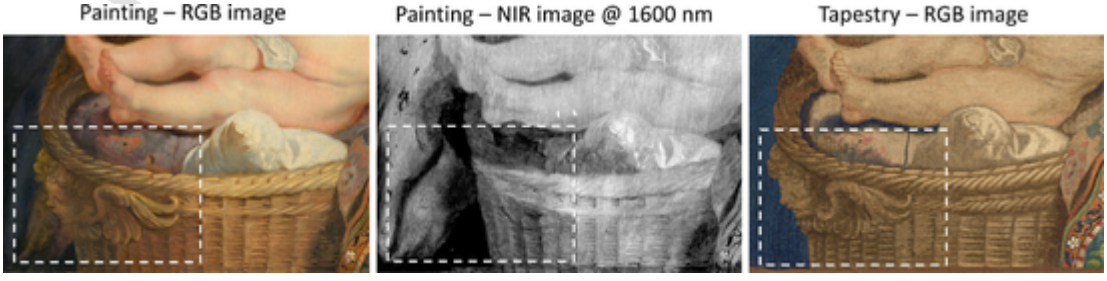

Fig. 2. Multispectral analysis of *Madonna della Cesta* painting by Rubens (RGB and NIR image) and tapestry by Févère (RGB image).

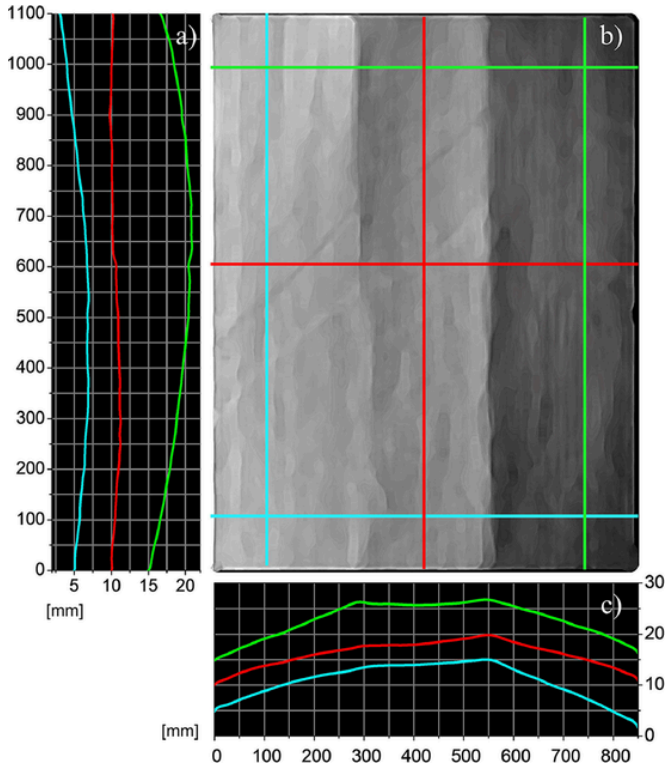

Fig. 3. 3D map of Rubens' wooden panel painting obtained from the autofocus acquisition of Vis-NIR scanner.

composing the painting's support may have been subject to different levels of stress, reflected by the surface's undulations and warps, which, in turn, affect its current appearance. Such deformations are quantified by the six profiles extracted from the topographic map along the vertical (Fig. 3a) and horizontal planes (Fig. 3c), and are highlighted by green, red, and light blue lines on the map (Fig. 3b). As shown below, the most relevant deformation peaks at a height of about 10 mm on the first and third panel, both vertically and horizontally, whereas the central panel displays a nearly flat surface.

4.2.2. Laser scanning microprofilometry

Micrometric mapping of the tapestry allowed for a morphological characterization of its fabrics, and, more specifically, its warp threads. Textile features were analysed using the three-dimensional data set generated by the laser scanning microprofilometer. Quota values of the analysed surface are displayed in dark violet and red on the colour scale (Fig. 4b) between 0 and 1 mm on the axial direction (Z axis). The texture micrometric shape may be observed in the raking light image (Fig. 4c). Thread sizes were measured on a scanning area of 12.5 mm^2 (Fig. 4b and c), by extracting 2D profiles (YZ axis, Z depth of 0.6 mm) that are orthogonal to the warp (as exemplified in Fig. 4a). Height and width of the threads resulted in the ranges of 0.8 - 1.2 mm and 0.2 - 0.6 mm, respectively.

4.2.3. 3D coloured models

When appraising a visible object, the human eye perceives both colour and shape simultaneously. When performing the instrumental diagnosis of an artwork, however, 3D and colour acquisition are almost invariably [29] carried out with different devices and at different points in time. Indeed, one single output is not exhaustive: the 3D model, albeit containing the whole shape information, lacks any reference to the colour appearance, while the colour image cannot provide any morphological information. Therefore, only through the overlap of the 3D model, either as point cloud or triangulated surface, and the relevant colour image, it is possible to facilitate the interpretation of the results, as well as improving the data analysis. The exact correlation between the 3D model and the relevant colour information allows for a straightforward identification of the measured features. Fig. 5 shows an example of this merging, through which the ripple corresponding to any given yarn may be exactly located. A video clip illustrating the whole process is available at the link provided below (Fig. 5).

4.3. Textiles characterization - Fibre optics reflectance spectroscopy (FORS)

The tapestry was analysed via near infrared spectroscopy to investigate the distribution of silk and wool, which were traditionally used by Févère to create shine and matte effects on tapestries, as reported in the literature [3]. Previous studies [8] have attested that natural fibres exhibit spectral features in the 2100 - 2400 nm spectral region, which correspond to the protein content of silk and wool. More specifically, vibrational features at 2205 nm (4535 cm^{-1}) and 2177 nm (4594

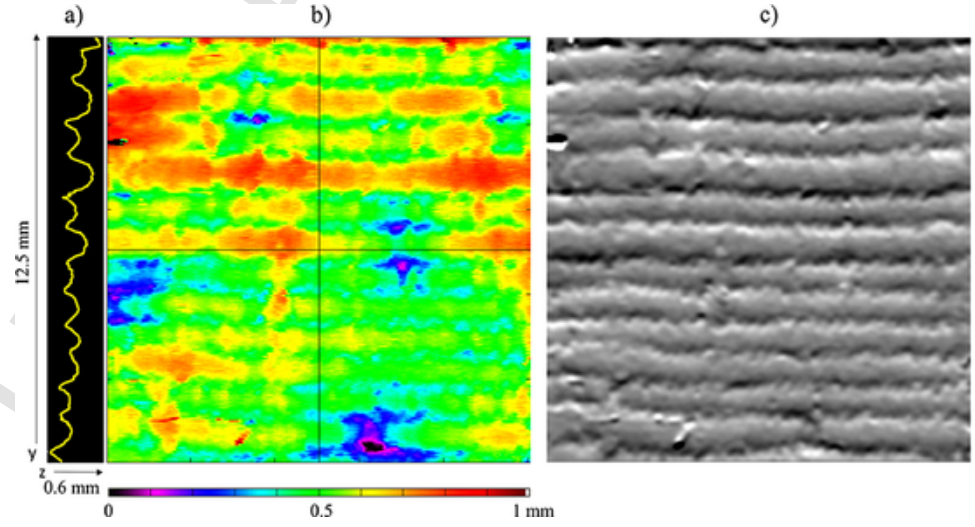

Fig. 4. Laser scanning microprofilometry: a) XZ profile showing the threads' size; b) topographic map displaying quota values in colour scale (0–1 mm scale bar); c) raking light b/w image.

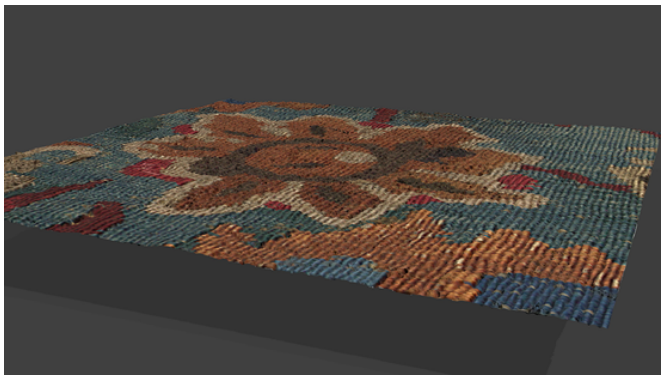

Fig. 5. 3D colour model of Févère's tapestry showing a detail of the flower's motif (area: 10 × 10 cm). The rendering can be observed in the linked video (link).

cm^{-1}) may be attributed to the β-sheet structure of silk and the α-helical structure of wool, respectively. Overtones in the 1500 - 1600 nm range have also been found to be a useful marker for β-sheet and α-helix content [9].

A set of wool and silk samples provided by OPD was used as reference in order to identify the main discriminating features of materials weaved in the tapestry. As expected, three absorption features consistent with the proteins' secondary structure of wool and silk were detected (Fig. 6a): an absorption at 1507 nm associated with the α-helix structure of wool, and two narrow absorptions at 1536 and 1575 nm attributed to the amide group of silk's β-sheet. For a straightforward differentiation between the two natural fibres, a reflectance value ratio measured at 1507, 1575 and 1536 nm was used. As displayed in Fig. 6b, the R_{1536}/R_{1575} ratio shows similar values for silk and wool fibres, whereas R_{1507}/R_{1575} and R_{1507}/R_{1536} ratios yield different values for each material, thus serving as effective indicative markers to overcome the variability of absolute reflectance factor values. In line with the restorers' indication, the presence of the two proteinaceous materials in areas of interest on the tapestry was thus investigated through the acquisition of 65 reflectance spectra. The above-mentioned ratio values, together with those measured on the reference samples, were plotted together (Fig. 6c), resulting in two distinct clusters of data, with silk displayed as blue squares and wool as red dots (full for the tapestry and empty for the reference samples). The non-invasive discrimination between wool and silk on the tapestry may provide crucial information in case of restoring interventions involving the reconstruction of missing parts.

4.4. Pigments distribution and identification

Spectral correlation maps (SCM) were computed on the spectral images acquired with the multispectral scanner, in order to visualize the distribution of pigments on the painted surface while also indicating similarities and differences in the colour palettes used by the two artists. The SCM of the painting and the tapestry are shown in Fig. 7. Processing was performed with a dedicated software, by applying a similarity criterion of similarity between the spectral image and a reference spectrum, extracted from the same Vis-NIR dataset. The comparison is shown in the graph in Fig. 7 and was based on six reference spectra, which were extracted in correspondence of red, green, and blue areas selected on both artworks (yellow asterisks on the RGB images in Fig. 7). SCMs based on reference spectra 1A and 1B show similarities in the distribution of red pigment, which was used for the clothing of the Virgin Mary in both artworks. The same pigment was probably used in mixed solution for flesh tones in Rubens' painting and for the carpet in Févère's tapestry. As evidenced by the SCM 1B, Rubens employed a green pigment in a small portion of the painting for Saint Ann's clothing, whereas Févère used a mixture of blue and yellow dyes to obtain a green hue in a number of areas, as confirmed by SCMs 2B and 3B, which are in perfect agreement. Those same areas on the painting show a different distribution of blue and green pigments (SCMs 2A, 3A).

A preliminary insight into the composition of the pigments and colorants was provided by Raman spectroscopy, which revealed that blue colours were realized with indigo and Lapis lazuli in the tapestry and painting, respectively (Fig. 8a and b).

The blue colourant in the tapestry is identified as indigo by the following values: 1573 cm^{-1} attributed to the stretching of conjugated groups $C = C$, $C = O$ and N—H; 1310 cm^{-1} due to the stretching of C—H (ν CC ring6 + ρ CH, asym); and 544 cm^{-1} due to bending vibrations involving the central $C = C$ coordinate [30]. The blue pigment in the oil painting was identified as Lapis lazuli mainly by 545 cm^{-1} assigned to the $\nu_1(S_3)$ symmetric stretching vibration and its overtone ($3\nu_1$) at 1639 cm^{-1} [31]. Moreover, the co-presence of indigo is ascertained by bands at 1575, 1310, 1014, 757, 574 cm^{-1} [30]. Other Raman lines, often overlapping, in the complex spectrum in Fig. 8b are attributable to white lead (ν_{sym} (CO_3^{2-}) at 1052 cm^{-1}) and calcite (C–O bond ν_{sym} (CO_3^{2-}) at 1086 cm^{-1} and in-plane bend ν_4 at 713 cm^{-1}). The presence of metal soaps may be deduced by broad and not well resolved bands at 1460–1410 cm^{-1} attributable to $\delta(CH_2)$, other bands at lower wavenumbers (760, 674 cm^{-1}) may be ascribed to δ(COO) or metal-oxygen vibrations. [32] The aliphatic C—H stretching vibrations between 2923 and 2854 cm^{-1} were observed (not reported), attributable to both metal soaps and drying oil [33].

5. Conclusions

A comprehensive analysis of Rubens' painting and Févère's tapestry was carried out through the combined application of a number of non-invasive techniques, allowing for the acquisition of iconographic, morphological, structural, and compositional information.

The geometric overlap of multi-spectral images provides evidence of the significant iconographic correspondence between the two artworks,

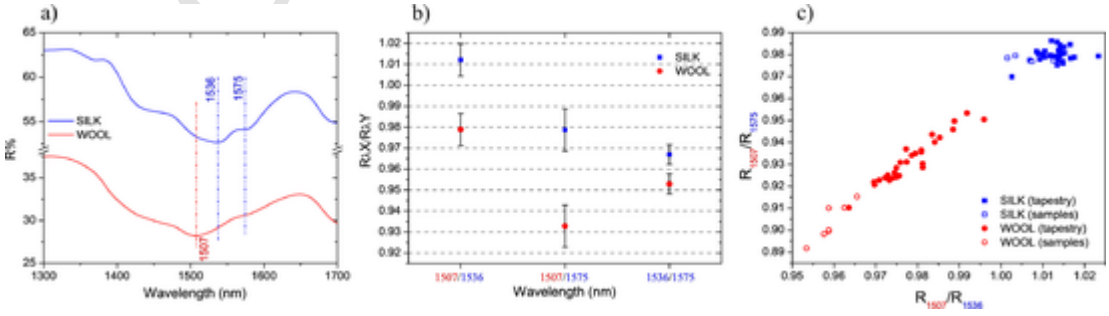

Fig. 6. Near infrared Fibre Optics Reflectance Spectroscopy: a) silk and wool reflectance spectra (blue and red lines, respectively) with overtones highlighted at 1507, 1536, and 1575 nm; b) mean values of R_{1507}/R_{1575}, R_{1507}/R_{1536}, R_{1536}/R_{1575} ratios measured on reference samples for silk and wool identification; c) silk and wool clusters based on R_{1507}/R_{1575} and R_{1507}/R_{1536} ratios measured on tapestry and reference samples.

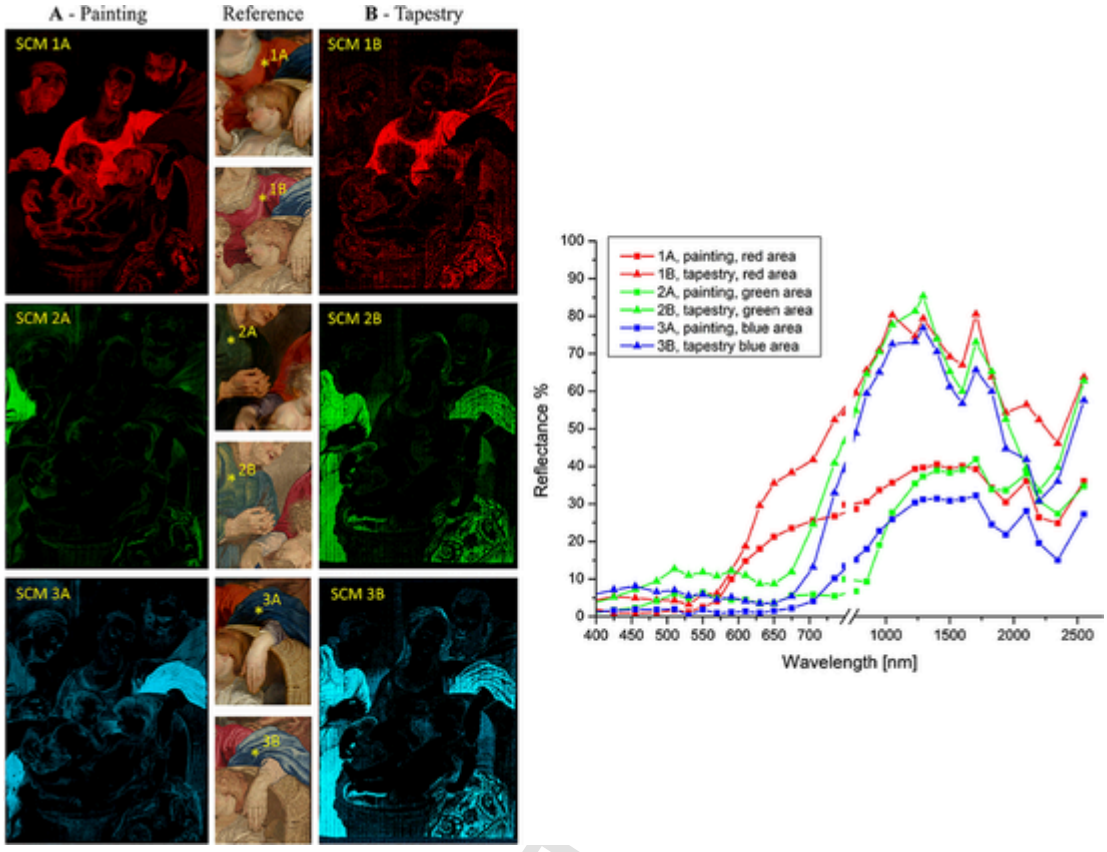

Fig. 7. Spectral correlation maps of the painting (SCM 1–3A) and the tapestry (SCM1-3B), computed by selecting three reference points (1A, 1B – red; 2A, 2B – green; 3A, 3B - blue) on three areas of interest, shown in the RGB images in the central column. The reflectance spectra of each selected point, obtained by multispectral scanning, are reported in the graph on the right.

suggesting that Fevère may have indeed referred to the same carton used by Rubens for his oil painting. The only appreciable difference revealed by NIR scanning concerns a detail in the painting at preparatory stage, namely a *pentimento*, which has no correspondence in the tapestry design at any stage or in the final version of Ruben's work.

Three-dimensional mapping of the painting surface allowed for the quantification of warps and deformations characterizing the painting's wooden support and affecting its current appearance. The tapestry's fabrics, and, more specifically, the warp threads, were morphological investigated by means of micrometric mapping. Colour information combined with the topographic maps resulted in the exact correlation of the measured 3D features with the RGB images. Such structural and morphological characterization may prove useful for conservation and restoration purposes.

The use of silk and wool by Févère to create shine and matte effects was also investigated by means of near infrared spectroscopy, based on the detection of overtones of vibrational features in the 1500 - 1600 nm range. The ratio between the measured reflectance values in this representative range was used to discriminate between the two materials. The identification and distinction of the tapestry's fabrics is significant, not only for historical documentation purposes, but also in view of restoring interventions involving the reconstruction of missing parts.

Further comparisons included in our analysis focused on pigments distribution, which was investigated by means of spectral correlation mapping. Results showed a good correspondence between the two artworks in terms of colour distribution of red pigments, while numerous differences were observed as regards the distribution of green and blue pigments. More specifically, green areas in Rubens' painting seem to result from the use of a pure green pigment, while Févère's green is more likely to be a mixture of blue and yellow dyes. Finally, a preliminary analysis of the composition of pigments carried out on the blue areas via Raman spectroscopy revealed a further difference, namely the use of indigo in the tapestry and Lapis lazuli in the painting. For a full characterization of Rubens and Févère's palettes further analysis is required, in order to identify all pigments and dyes.

Declaration of Competing Interest

There are no conflicts to declare.

Acknowledgements

This research was funded by the EU Community's H2020 - Research Infrastructure programme under the IPERION CH Project (GA n. 654028).

The authors would like to thank M.C. Gigli, G. Bacci and Lucia Meoni for the fruitful discussions and the Director of the Galleria Uffizi, Eike Schmidt, for granting us permission to analyse the artworks.

Diego Sali from Bruker Italia is acknowledged for performing the measurements with Raman Bruker Bravo Spectrophotometer.

Supplementary materials

Supplementary material associated with this article can be found, in the online version, at doi:10.1016/j.microc.2019.104472.

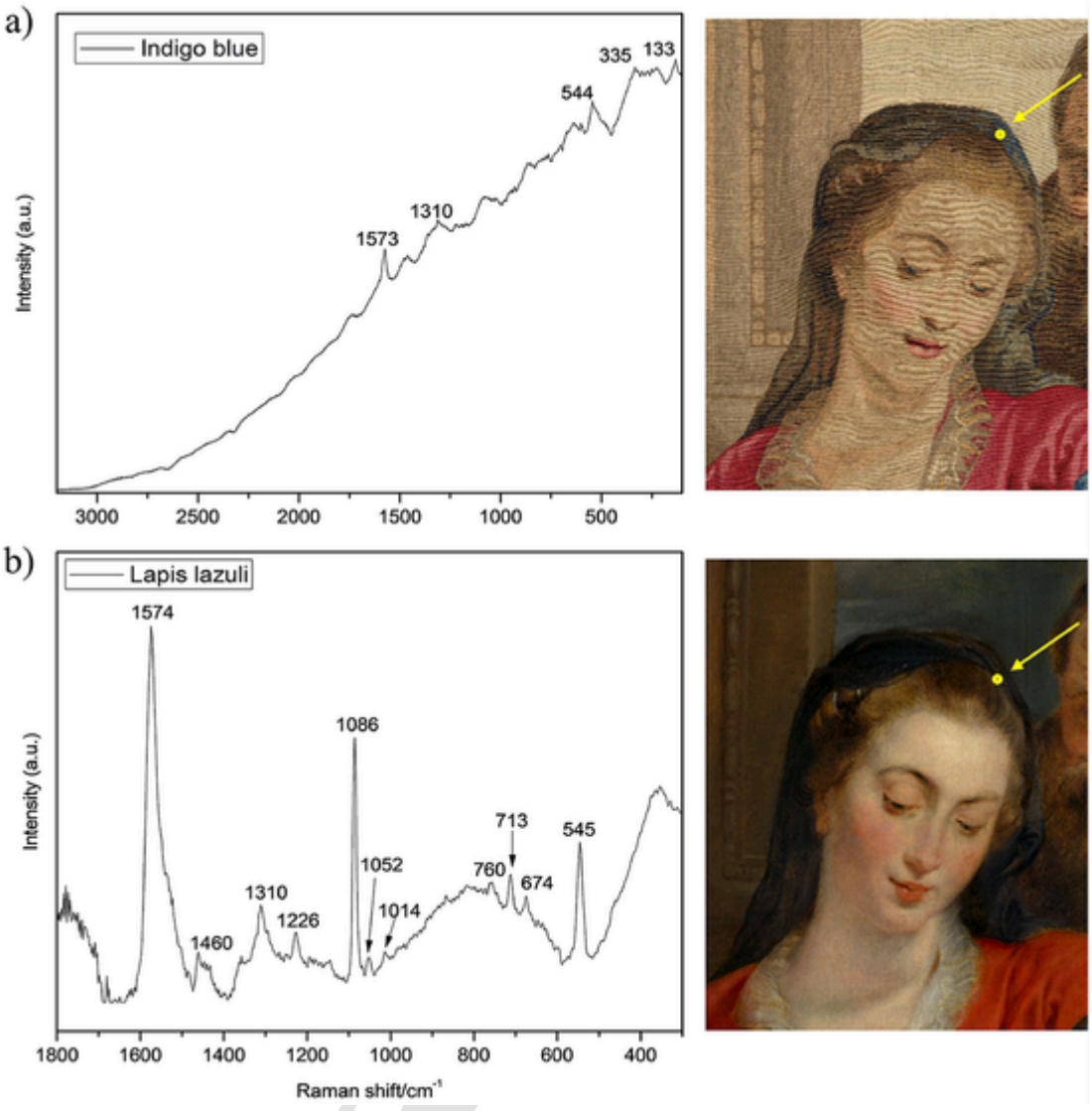

Fig. 8. Raman spectra acquired on blue portions of the tapestry (a) and painting (b) revealing indigo and lapis lazuli composition, respectively. Point of spectra acquisition highlighted in yellow in the RGB images on the right.

References

[1] C. Conti, Ricerche Storiche Sull'arte Degli Arazzi in Firenze, Sansoni, Firenze, 1876.

[2] L. Meoni, Gli Arazzi Nei Musei Fiorentini, La Collezione Medicea - Catalogo Completo, Sillabe, Firenze, 2018.

[3] R. Spinelli, La Grande Storia Dell'artigianato, 5, Giunti, Firenze, 2003.

[4] A. Baran, A. Fiedler, H. Schulz, M. Baranska, In situ raman and IR spectroscopic analysis of indigo dye, Anal. Methods 2 (2010) 1372–1376, doi:10.1039/C0AY00311E.

[5] I. Degano, J.J. Łucejko, M.P. Colombini, The unprecedented identification of safflower dyestuff in a 16th century tapestry through the application of a new reliable diagnostic procedure, J. Cult. Herit. 12 (2011) 295–299.

[6] L.G. Angelini, S. Tozzi, S. Bracci, F. Quercioli, B. Radicati, M. Picollo, Characterization of traditional dyes of the mediterranean area by non-invasive UV–Vis-NIR reflectance spectroscopy, Stud. Conserv. 55–2 (2010) 184–189, doi:10.1179/sic.2010.55.supplement-2.184.

[7] F. Lennard, Preserving image and structure: tapestry conservation in Europe and the United States, Stud. Conserv. 51 (2006) 43–53, doi:10.1179/sic.2006.51.Supplement-1.43.

[8] J.K. Delaney, P. Ricciardi, L. Glinsman, M. Palmer, J. Burke, Use of near infrared reflectance imaging spectroscopy to map wool and silk fibres in historic tapestries, Anal. Methods 8 (2016) 7886, doi:10.1039/c6ay02066f.

[9] X. Zhang, P. Wyeth, Moisture sorption as a potential condition marker for historic silks: noninvasive determination by near-infrared spectroscopy, Appl. Spectrosc. 61 (2007) 2, doi:10.1366/000370207779947611.

[10] R. Fontana, M.C. Gambino, M. Greco, L. Marras, M. Materazzi, E. Pampaloni, A. Pelagotti, L. Pezzati, P. Poggi, C. Sanapo, 2D and 3D optical diagnostic techniques applied to madonna dei fusi by leonardo da vinci, Proc. SPIE 5857, 2005, pp. 166–176.

[11] R. Fontana, M. Barucci, E. Pampaloni, J. Striova, L. Pezzati, From leonardo to raffaello: insights by vis-ir reflectography, acta artis academica, Interpretation of Fine Art's Analysis in Diverse Contexts 2014, Praga, 2014.

[12] C. Daffara, E. Pampaloni, L. Pezzati, M. Barucci, R. Fontana, Scanning multispectral IR reflectography SMIRR: an advanced tool for art diagnostics, Acc. Chem. Res. 43 (2010) 847–856, doi:10.1021/ar900268t.

[13] E.W. Rosolowsky, A.A. Goodman, D.J. Wilner, J.P. Williams, The spectral correlation function: A new tool for analyzing spectral line maps, ApJ. 524 (1999) 887–894, doi:10.1086/307863.

[14] M. Picollo, M. Bacci, A. Casini, F. Lotti, S. Porcinai, B. Radicati, L. Stefani, Fiber optics reflectance spectroscopy: A non-destructive technique for the analysis of works of art, in: Martellucci (Ed.), Optical Sensors and Microsystems: New Concepts, Materials, Technologies, Kluwer Academic/Plenum Publishers, New York, 2000.

[15] L. Burgio, R. Clark, Library of FT-Raman spectra of pigments, minerals, pigment media and varnishes, and supplement to existing library of raman spectra of pigments with visible excitation, Spectrochim. Acta. Part A 57 (2001) 1491–1521, doi:10.1016/S1386-1425(00)00495-9.

[16] C. Bonifazzi, P. Carcagnì, R. Fontana, M. Greco, M. Mastroianni, M. Materazzi, E. Pampaloni, L. Pezzati, D. Bencini, A scanning device for Vis-NIR multispectral imaging of paintings, J. Opt. A Pure Appl. Opt. 10 (2008), doi:10.1088/1464-4258/10/6/064011 064011.

[17] P. Carcagnì, P.A. Della, R. Fontana, M. Greco, M. Mastroianni, M. Materazzi, E. Pampaloni, L. Pezzati, Multispectral imaging of paintings by optical scanning, Opt. Lasers Eng. 45 (2007) 360–367, doi:10.1016/j.optlaseng.2005.02.010.
[18] in ed. byR. Fontana, M. Barucci, P. Carcagnı`, C. Daffara, E. Pampaloni, L. Pezzati, Autofocus laser system for multi-NIR scanning imaging of painting surfaces, in: L. Pezzati, R. Salimbeni (Eds.), SPIE Proceeding, Optics for Arts, Architecture, and Archaeology III, 2011, p. 8084 8084051-9R.
[19] P. Carcagnì, C. Daffara, R. Fontana, M.C. Gambino, M. Mastroianni, C. Mazzotta, E. Pampaloni, L. Pezzati, Optical microprofilometry for archaeology, Proc. SPIE 5857, 2005, pp. 118–128.
[20] R. Fontana, C. Mazzotta, M.C. Gambino, M. Greco, E. Pampaloni, L. Pezzati, High-resolution 3D survey of artworks, Proc. SPIE 5457, 2004, pp. 719–726.
[21] E. Pampaloni, R. Bellucci, P. Carcagnì, A. Casaccia, R. Fontana, M.C. Gambino, R. Piccolo, P. Pingi, L. Pezzati, Three-dimensional survey of paint layer, Proc. SPIE 6618, 2007, pp. 1–10.
[22] R.G. Kuehni, Color: An Introduction to Practice and Principles, Wiley, New York, USA, 1997.
[23] F. Pozzi, E. Basso, A. Rizzo, A. Casaratto, T.J. Tague, Evaluation and optimization of the potential of a handheld raman spectrometer: in situ, noninvasive materials characterization in artworks, J. Raman Spectrosc. (2019) 1–12, doi:10.1002/jrs.5585.
[24] F.A. Kruse, A.B. Lefkoff, J.W. Boardman, K.B. Heidebrecht, A.T. Shapiro, P.J. Barloon, A.F.H. Goetz, The spectral image processing system (SIPS) – Interactive visualization and analysis of imaging spectrometer data, Remote Sens. Environ. 44 (1993) 145–163, doi:10.1016/0034-4257(93)90013-N.
[25] SIPS user's guide, spectral image processing system, Version 1.2, Center for the Study of Earth from Space (CSES), Boulder, CO, 1992, p. 88.
[26] M. Kazhdan, H. Hoppe, Screened poisson surface reconstruction, ACM Trans. Graphics 32 (3) (2013).
[27] P. Cignoni, M. Callieri, M. Corsini, M. Dellepiane, F. Ganovelli, G. Ranzuglia, MeshLab: an open-source mesh processing tool, Eurographics Italian Chapter Conference, 2008, pp. 129–136.
[28] M. Corsini, M. Dellepiane, F. Ponchio, R. Scopigno, Image-to-Geometry registration: A mutual information method exploiting illumination-related geometric properties, Pacific Graphics 28 (7) (2009), doi:10.1111/j.1467-8659.2009.01552.x.
[29] M. Guarneri, M. Ferri De Collibus, G. Fornetti, M. Francucci, M. Nuvoli, R. Ricci, Remote colorimetric and structural diagnosis by RGB-ITR color laser scanner prototype, Adv. Opt. Technol. 512902 (2012) 1–6 1–6, doi:10.1155/2012/512902.
[30] A. Baran, A. Fiedler, H. Schulz, M. Baranska, In situ raman and IR spectroscopic analysis of indigo dye, Anal. Methods 2 (2010) 1372–1376, doi:10.1039/c0ay00311e.
[31] N. Buzgar, A. Buzatu, A. Apopei, V. Cotiuga, In situ raman spectroscopy at the voronet¸ Monastery (16th century, Romania): new results for green and blue pigments, Vib. Spectrosc. 72 (2014) 142–148.
[32] V. Otero, D. Sanches, C. Montagner, M. Vilarigues, L. Carlyle, J.A. Lopes, M.J. Melo, Characterisation of metal carboxylates by raman and infrared spectroscopy in works of art, J. Raman Spectrosc. 45 (2014) 1197–1206, doi:10.1002/jrs.4520.
[33] A. Schönemann, H.G.M. Edwards, Raman and FTIR microspectroscopic study of the alteration of Chinese tung oil and related drying oils during ageing, Anal. Bioanal. Chem. 400 (2011) 1173–1180, doi:10.1007/s00216-011-4855-0.